

# Precision determination of the small- $x$ gluon from charm production at LHCb

Rhorry Gauld<sup>1,2,\*</sup> and Juan Rojo<sup>3,4,†</sup>

<sup>1</sup>*Institute for Theoretical Physics, ETH, CH-8093 Zurich, Switzerland*

<sup>2</sup>*Institute for Particle Physics Phenomenology, University of Durham, DH1 3LE Durham, United Kingdom*

<sup>3</sup>*Department of Physics and Astronomy, VU University Amsterdam,*

*De Boelelaan 1081, NL-1081, HV Amsterdam, The Netherlands*

<sup>4</sup>*Nikhef, Science Park 105, NL-1098 XG Amsterdam, The Netherlands*

(Dated: December 9, 2024)

The small- $x$  gluon in global fits of parton distributions is affected by large uncertainties from the lack of direct experimental constraints. In this work we provide a precision determination of the small- $x$  gluon from the exploitation of forward charm production data provided by LHCb for three different centre-of-mass (CoM) energies: 5 TeV, 7 TeV and 13 TeV. The LHCb measurements are included in the PDF fit by means of normalized distributions and cross-section ratios between data taken at different CoM values,  $R_{13/7}$  and  $R_{13/5}$ . We demonstrate that forward charm production leads to a reduction of the PDF uncertainties of the gluon down to  $x \simeq 10^{-6}$  by up to an order of magnitude, with implications for high-energy colliders, cosmic ray physics and neutrino astronomy.

The determination of the internal structure of the proton, as encoded by the non-perturbative parton distribution functions (PDFs) [1–3], has far-reaching implications for many areas in nuclear, particle and astroparticle physics. A topic that has recently attracted substantial interest is the determination of the gluon PDF at small- $x$ , which is of direct relevance for the modelling of soft QCD at the LHC [4], neutrino astronomy [5–8] and cosmic ray physics [9], as well as for future lepton-proton [10] and proton-proton higher-energy colliders [11]. Constraints on the gluon PDF from deep-inelastic scattering (DIS) inclusive and charm structure functions at HERA [12, 13] are limited to  $x \gtrsim 3 \cdot 10^{-5}$  in the perturbative region, and consequently for smaller values of  $x$  there are large uncertainties from the lack of direct experimental information.

Last year, it was realized [14–16] that a way forward was provided by considering inclusive  $D$  meson production in  $pp$  collisions at the LHC, for which the LHCb experiment had already provided data at 7 TeV [17]. The inclusive charm cross-section at the LHC is dominated by heavy quark pair production, in turn driven by the gluon-gluon luminosity, and the forward LHCb kinematics allow a coverage of the small- $x$  region that can reach as low as  $x \simeq 10^{-6}$ . While the direct inclusion of absolute  $D$  meson cross-sections into a PDF fit is unfeasible due to the large theory uncertainties that affect the NLO calculation, it has been demonstrated [14, 15] that by using tailored normalized distributions it is possible to exploit the LHCb measurements to achieve a significantly improved description of the small- $x$  gluon. A complementary approach, suggested in [16], would be to include  $D$  meson data into PDF fits with the use of ratios of cross-sections between different center-of-mass (CoM) energies,

which benefit from various uncertainty cancellations [18].

More recently, the LHCb collaboration has presented the analogous  $D$  meson cross-section measurements at  $\sqrt{s} = 5$  and 13 TeV [19, 20], together with the corresponding ratios  $R_{13/7}$  and  $R_{13/5}$ .<sup>1</sup> In this letter, we quantify the impact of the LHCb  $D$  meson data at different CoM energies on the small- $x$  gluon from the NNPDF3.0 global analysis [21]. These data are included both in terms of normalized cross-sections as well as by means of the cross-section ratio measurements. Our strategy leads to a precision determination of the small- $x$  gluon, substantially improving previous results, and highlighting the consistency of the LHCb measurements at the three CoM energies. We illustrate the implications of our results for ultra high-energy (UHE) neutrino-nucleus cross-sections  $\sigma_{\nu N}(E_\nu)$ , and the longitudinal structure function  $F_L(x, Q^2)$  at future lepton-proton colliders.

The LHCb  $D$  meson production data is presented double differentially in transverse momentum ( $p_T^D$ ) and rapidity ( $y^D$ ) for a number of final states,  $D^0$ ,  $D^+$ ,  $D_s^+$  and  $D^{*+}$ , which also contain the contribution from charge-conjugate states. To include these measurements into the global PDF fit, we define two observables:

$$N_X^{ij} = \frac{d^2\sigma(X \text{ TeV})}{dy_i^D d(p_T^D)_j} \bigg/ \frac{d^2\sigma(X \text{ TeV})}{dy_{\text{ref}}^D d(p_T^D)_j}, \quad (1)$$

$$R_{13/X}^{ij} = \frac{d^2\sigma(13 \text{ TeV})}{dy_i^D d(p_T^D)_j} \bigg/ \frac{d^2\sigma(X \text{ TeV})}{dy_i^D d(p_T^D)_j}, \quad (2)$$

which benefit from the partial cancellation of the residual scale dependence from missing higher-orders, while retaining sensitivity to the gluon since different regions of  $x$  are probed in the numerator and denominator of

\*Electronic address: rgauld@phys.ethz.ch

†Electronic address: j.rojo@vu.nl

<sup>1</sup> The LHCb 13 TeV data considered here accounts for the recently released erratum [20], which primarily affected low- $p_T$   $D^0$  data.

these observables. The ratio measurements,  $R_{13/7}$  and  $R_{13/5}$ , are available for  $y^D \in [2.0, 4.5]$  in five bins and for  $p_T^D \in [0, 8]$  GeV in eight bins. The 5 TeV and 13 TeV absolute cross section measurements extend to higher  $p_T^D$  values, however these additional points are excluded from the fit since they might be affected by large logarithmic contributions [22]. The reference rapidity bin in the normalized distributions  $N_X^{ij}$  in Eq. (1) is chosen to be  $y_{\text{ref}}^D \in [3.0, 3.5]$ , as in [15], since we have verified that this choice maximizes the cancellation of scale uncertainties for the considered data. We restrict our analysis to the  $\{D^0, D^+, D_s^+\}$  final states, except for 7 TeV where the  $D_s^+$  data, with large uncertainties, is not considered.

The theoretical predictions for  $D$  meson production are computed at NLO+PS accuracy using POWHEG [23–25] to match the fixed-order calculation [26] to the PYTHIA8 shower [27, 28] with the MONASH 2013 tune [4]. The POWHEG results have previously been shown to be consistent [14, 29] with both the NLO+PS (a)MC@NLO [30, 31] method and the semi-analytic FONLL calculation [32, 33]. The NNPDF3.0 NLO set of parton distributions with  $\alpha_s(m_Z) = 0.118$ ,  $N_f = 5$  and  $N_{\text{rep}} = 1000$  replicas has been used, interfaced with LHAPDF6 [34]. The internal POWHEG routines have been modified to extract  $\alpha_s$  from LHAPDF6, and the compensation terms [32] to consistently match the  $N_f = 5$  PDFs with the fixed-order  $N_f = 3$  calculation [26] are included. Other settings of the theory calculation, such as the values for fragmentation fractions, are the same as those in [14]. The central value for the charm quark pole mass is taken to be  $m_c = 1.5$  GeV, following the HXSWG recommendation [35], and the renormalization and factorization scales are set equal to the heavy quark transverse mass in the Born configuration,  $\mu = \mu_R = \mu_F = \sqrt{m_c^2 + p_T^2}$ .

The impact of the LHCb  $D$  meson data on the NNPDF3.0 small- $x$  gluon can be quantified using the Bayesian reweighting technique [36, 37]. We have studied separately the impact of the three data sets of normalized distributions,  $N_5$ ,  $N_7$  and  $N_{13}$  and the two cross-section ratios,  $R_{13/5}$  and  $R_{13/7}$ , as well specific combinations of these, always avoiding double counting. The experimental bin-by-bin correlation matrices are included for the cross-section ratios  $R_{13/X}$ , while for the normalized cross-section data, where the experimental correlation matrix is only available for  $N_5$  and  $N_{13}$ , statistical and systematic uncertainties are added in quadrature.

We find that while NLO theory describes successfully the cross-section ratios  $R_{13/7}$  and  $R_{13/5}$  and the majority of the data points that compose the normalized distributions  $N_5$ ,  $N_7$  and  $N_{13}$ , poorer agreement is found for a number of points in the  $D^0$  final state at both 5 and 13 TeV, in particular for those which are farthest from the reference rapidity bin  $y_{\text{ref}}^D$ . Note also that the  $D^0$  final state is the one that exhibits the smallest experimental uncertainties. This may indicate the need for the full NNLO calculation, so far available only for  $t\bar{t}$  produc-

tion [38]. To avoid this problem, for the  $N_5$  and  $N_{13}$   $D^0$  final state we impose kinematic cuts and restrict the fitted data set to those points in neighboring rapidity bins of  $y_{\text{ref}}^D$ . We have verified (see Fig. 3) that our results are stable with respect the specific choice of  $y_{\text{ref}}^D$ .

To illustrate the good agreement found for the considered LHCb data and the corresponding NLO theory predictions, we compute the  $\chi^2/N_{\text{dat}}$  for each of the five datasets, for different combinations of data used as input in the PDF fit. These results are summarized in Table I, where the data that has been included in each case are highlighted in boldface, and the number in brackets indicates  $N_{\text{dat}}$  for each data set.

$N_5(70)$	$N_7(59)$	$N_{13}(106)$	$R_{13/5}(107)$	$R_{13/7}(75)$
<b>1.01</b>	0.65	0.92	1.48	0.95
1.47	<b>0.89</b>	1.34	1.50	0.94
1.09	0.68	<b>0.97</b>	1.49	0.94
1.15	0.73	1.09	<b>1.41</b>	0.96
1.44	0.87	1.30	1.46	<b>0.93</b>
<b>1.05</b>	0.67	0.95	1.48	<b>0.95</b>
0.98	<b>0.64</b>	0.91	<b>1.45</b>	0.96
<b>1.14</b>	<b>0.7</b>	<b>1.01</b>	1.49	0.94

TABLE I: The  $\chi^2/N_{\text{dat}}$  for the LHCb  $D$  meson measurements considered,  $N_5$ ,  $N_7$ ,  $N_{13}$ ,  $R_{13/7}$  and  $R_{13/5}$ , for various combinations of input to the PDF fit (highlighted in boldface).

We find that the normalized distributions,  $N_5$ ,  $N_7$  and  $N_{13}$ , as well as the ratio  $R_{13/5}$ , have a similar substantial pull on the gluon, both for central values and for the reduction of the PDF uncertainty. The  $R_{13/7}$  ratio pulls the small- $x$  gluon in the same direction but with less constraining power. This is demonstrated in Fig. 1 where we show the  $1-\sigma$  relative PDF uncertainties for the gluon at  $Q^2 = 4$  GeV<sup>2</sup> in NNPDF3.0 and in the subsequent fits when the various LHCb  $D$  meson data sets are included.

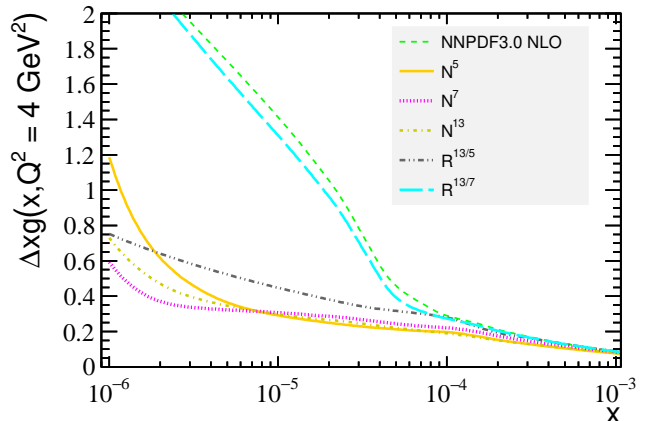


FIG. 1: The  $1-\sigma$  relative PDF uncertainties for the small- $x$  gluon at  $Q^2 = 4$  GeV<sup>2</sup> in NNPDF3.0 and in the subsequent fits when the LHCb charm data are included one at a time.

In the following we show results for two representative combinations of the LHCb measurements, namely  $N_7 + R_{13/5}$  and  $N_5 + N_7 + N_{13}$ . In Fig. 2 we compare the small- $x$  gluon in NNPDF3.0 with the resultant gluon in these two cases, as well as the central value from the  $N^5 + R^{13/7}$  fit. The central value of the small- $x$  gluon is consistent for all three combinations, down to  $x \simeq 10^{-6}$ , and, as expected from Fig. 1, we observe a dramatic reduction of the  $1\text{-}\sigma$  PDF uncertainties. We have verified that these updated results are consistent with our original study [14] (GRRT), yet significantly more precise, see Fig. 5 below.

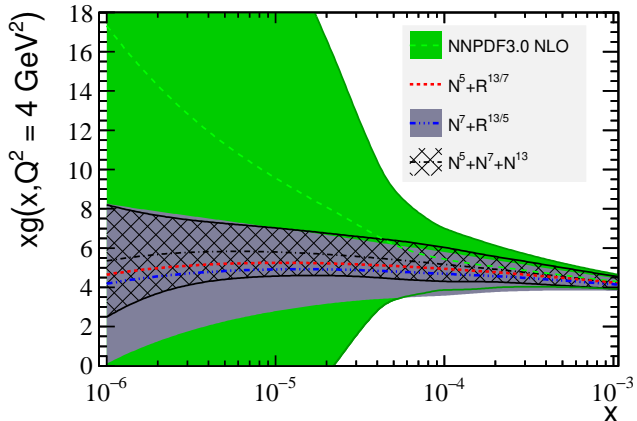


FIG. 2: The NLO gluon in NNPDF3.0 and for various combinations of LHCb data included, at  $Q^2 = 4 \text{ GeV}^2$ .

Given the sizeable theory errors that affect charm production, it is important to assess the robustness of our results with respect to the scale variations of the NLO calculation as well as with the value of  $m_c$ . We thus have quantified how the resultant gluon are affected by theory variations, including:  $\mu = \sqrt{4m_c^2 + p_T^2}$ , alternative reference bins  $y_{\text{ref}}^{D^0} = [2.5, 3.0]$  and  $[3.5, 4.0]$ , and charm mass variations of  $\Delta m_c = 0.2 \text{ GeV}$ . The resultant central values of the gluon are shown in Figs. 3 and 4, compared with NNPDF3.0 and with the  $1\text{-}\sigma$  PDF uncertainty band from the  $N_5 + N_7 + N_{13}$  and  $N_7 + R_{13/5}$  fits, respectively.

We find that our results are reasonably stable upon these variations of the input theory settings, in particular for the  $N^7 + R^{13/5}$  fits, highlighting that the cancellation of theory errors is more effective for the cross-section ratios than for the normalized distributions. Even for the most constraining combination, the  $N_5 + N_7 + N_{13}$  fits, all theory variations are contained within the 95% confidence level interval of the PDF uncertainty. This study demonstrates that the sizable reduction of the small- $x$  gluon PDF errors is robust with respect to theoretical uncertainties. A further reduction of the scale dependence could only be achieved by the full NNLO calculation.

Our precision determination of the small- $x$  gluon has important phenomenological implications, which we choose to illustrate with two representative examples: the longitudinal structure function  $F_L$  at a future high-

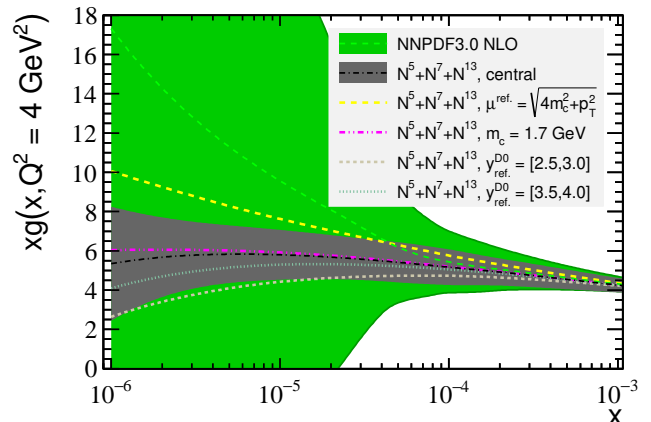


FIG. 3: Dependence of the small- $x$  gluon from the  $N_5 + N_7 + N_{13}$  fits for variations in the input theory settings.

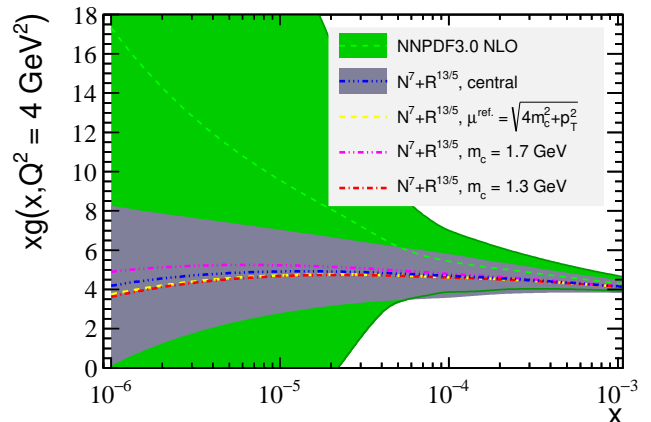


FIG. 4: Same as Fig. 3 for the  $N^7 + R^{13/5}$  fits.

energy lepton-proton collider, and the UHE neutrino-nucleus cross-section. First of all, we have computed  $F_L(x, Q^2)$  for  $Q^2 = 3.5 \text{ GeV}^2$  using APFEL [39] in the FONLL-B general mass scheme [40]. The proposed Large Hadron electron Collider (LHeC) would be able to measure  $F_L$  down to  $x \gtrsim 10^{-6}$  with few percent precision for  $Q^2 \gtrsim 2 \text{ GeV}^2$  [10], hence providing a unique probe of BFKL resummations and non-linear QCD dynamics [41]. In Fig. 5 we compare  $F_L$  computed with NNPDF3.0 and with the results of this work, as well as with the original GRRT calculation. We observe that the PDF uncertainties on  $F_L$  at  $x \simeq 10^{-6}$  are now reduced by almost order of magnitude, and that  $F_L$  itself is always positive for the  $x$  range accessible at the LHeC.

Next, we have computed the UHE charged-current (CC) neutrino-nucleus cross-section as a function of the incoming neutrino energy  $E_\nu$ , using a stand-alone code based on APFEL for the calculation of the NLO structure functions. At the highest values of  $E_\nu$  that might be accessible at neutrino telescopes such as IceCube [42] and KM3NET [43], the neutrino-nucleus interactions probes the quark sea PDFs at  $Q^2 \simeq M_W^2$  and down to  $x \simeq 10^{-8}$ ,

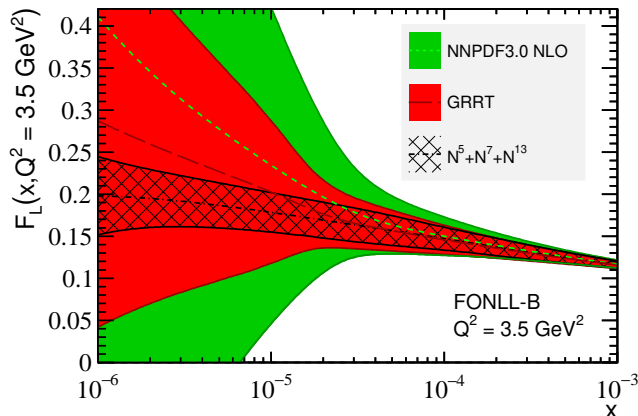


FIG. 5: The structure function  $F_L(x, Q^2)$  at  $Q^2 = 3.5 \text{ GeV}^2$ , comparing the NNPDF3.0 predictions both with the results of this work and with the GRRT calculation.

a region where the quark distributions are driven by the small- $x$  gluon by means of DGLAP evolution effects [44].

In Fig. 6 we compare the CC UHE neutrino-nucleus cross-section from NNPDF3.0 with the results of this work. As in the case of  $F_L$ , we find a sizable reduction of the PDF uncertainties, which are by far the dominant theory uncertainty for this process at high  $E_\nu$ . This way, NLO QCD provides a prediction accurate to  $\lesssim 10\%$  up to  $E_\nu \simeq 10^{12} \text{ GeV}$ , a region where a rather different behaviour are found in scenarios with non-linear QCD evolution effects [45]. Our results for the UHE cross-section are more precise than existing calculations [5, 46], based on PDF fits where the only constraints on the small- $x$  gluon come from the inclusive and charm HERA data, and therefore provide a clean handle to disentangle possible beyond the Standard Model effects in this process [47].

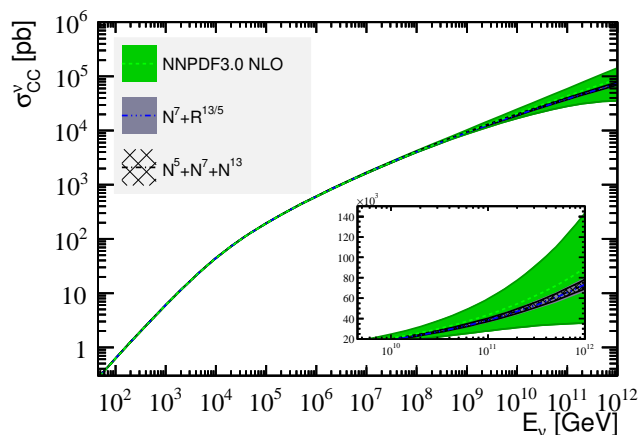


FIG. 6: The NLO charged-current neutrino-nucleus cross-section as a function of the neutrino energy  $E_\nu$ , computed with NNPDF3.0 and with the results of this work.

To summarize, in this work we have presented a precision determination of the small- $x$  gluon down to  $x \simeq 10^{-6}$

from LHCb charm production in the forward region at  $\sqrt{s} = 5, 7$  and  $13 \text{ TeV}$ . We have shown that the LHCb data provided at the three CoM energies leads to consistent constraints on the small- $x$  gluon, and have determined the combination that maximizes the reduction of PDF uncertainties, namely the sum of normalized distributions  $N^5 + N^7 + N^{13}$ . We have found indications that NLO QCD may not be adequate to describe the most precise data, a subset of points for the  $D^0$  final state at 5 and 13 TeV (here excluded by kinematical cuts), suggesting that NNLO corrections are required to exploit the full LHCb charm dataset.

We have illustrated how the improved small- $x$  gluon leads to significantly reduced theory uncertainties for  $F_L$  at future high-energy lepton-proton colliders and for the UHE neutrino-nucleus interactions. We have however only scratched the surface of the phenomenological implications of our work. It is important to explore these implications further to inform other applications, such as the modelling of semi-hard QCD processes at the LHC in Monte Carlo event generators and for calculations of cosmic ray production. Moreover, it would be interesting to compare our determination of the small- $x$  gluon with those that could be achieved from other processes with similar kinematical coverage, such as exclusive production [48] or forward photon production [49, 50].

The results of this work are available upon request in the form of LHAPDF6 grids [34].

*Acknowledgements.* We thank L. Rottoli and V. Bertone for the calculations of the UHE neutrino cross-sections and for assistance with APFEL. We are also grateful to Dominik Mueller and Alex Pearce for information with regards to the LHCb data. We acknowledge the support provided by the GridPP Collaboration. The work of J. R. is partially supported by an ERC Starting Grant ‘‘PDF4BSM’’.

- 
- [1] S. Forte and G. Watt, *Ann.Rev.Nucl.Part.Sci.* **63**, 291 (2013), 1301.6754.
  - [2] J. Butterworth et al., *J. Phys.* **G43**, 023001 (2016), 1510.03865.
  - [3] J. Rojo et al., *J. Phys.* **G42**, 103103 (2015), 1507.00556.
  - [4] P. Skands, S. Carrazza, and J. Rojo, *European Physical Journal* **74**, 3024 (2014), 1404.5630.
  - [5] A. Cooper-Sarkar, P. Mertsch, and S. Sarkar, *JHEP* **08**, 042 (2011), 1106.3723.
  - [6] M. V. Garzelli, S. Moch, and G. Sigl, *JHEP* **10**, 115 (2015), 1507.01570.
  - [7] R. Gauld, J. Rojo, L. Rottoli, S. Sarkar, and J. Talbert, *JHEP* **02**, 130 (2016), 1511.06346.
  - [8] A. Bhattacharya, R. Enberg, Y. S. Jeong, C. S. Kim, M. H. Reno, I. Sarcevic, and A. Stasto (2016), 1607.00193.
  - [9] D. d’Enterria, R. Engel, T. Pierog, S. Ostapchenko, and K. Werner, *Astropart. Phys.* **35**, 98 (2011), 1101.5596.

- [10] J. Abelleira Fernandez et al. (LHeC Study Group), *J.Phys.* **G39**, 075001 (2012), 1206.2913.
- [11] M. L. Mangano et al. (2016), 1607.01831.
- [12] H. Abramowicz et al. (H1 , ZEUS), *Eur.Phys.J.* **C73**, 2311 (2013), 1211.1182.
- [13] H. Abramowicz et al. (ZEUS, H1), *Eur. Phys. J.* **C75**, 580 (2015), 1506.06042.
- [14] R. Gauld, J. Rojo, L. Rottoli, and J. Talbert, *JHEP* **11**, 009 (2015), 1506.08025.
- [15] O. Zenaiev et al. (PROSA), *Eur. Phys. J.* **C75**, 396 (2015), 1503.04581.
- [16] M. Cacciari, M. L. Mangano, and P. Nason, *Eur. Phys. J.* **C75**, 610 (2015), 1507.06197.
- [17] R. Aaij et al. (LHCb), *Nucl.Phys.* **B871**, 1 (2013), 1302.2864.
- [18] M. L. Mangano and J. Rojo, *JHEP* **1208**, 010 (2012), 1206.3557.
- [19] R. Aaij et al. (LHCb) (2016), 1610.02230.
- [20] R. Aaij et al. (LHCb), *JHEP* **03**, 159 (2016), [Erratum: *JHEP*09,013(2016)], 1510.01707.
- [21] R. D. Ball et al. (NNPDF), *JHEP* **1504**, 040 (2015), 1410.8849.
- [22] M. Cacciari and M. Greco, *Nucl.Phys.* **B421**, 530 (1994), hep-ph/9311260.
- [23] P. Nason, *JHEP* **0411**, 040 (2004), hep-ph/0409146.
- [24] S. Frixione, P. Nason, and C. Oleari, *JHEP* **0711**, 070 (2007), 0709.2092.
- [25] S. Alioli, P. Nason, C. Oleari, and E. Re, *JHEP* **1006**, 043 (2010), 1002.2581.
- [26] S. Frixione, P. Nason, and G. Ridolfi, *JHEP* **0709**, 126 (2007), 0707.3088.
- [27] T. Sjostrand, S. Mrenna, and P. Z. Skands, *Comput. Phys. Commun.* **178**, 852 (2008), 0710.3820.
- [28] T. Sjöstrand, S. Ask, J. R. Christiansen, R. Corke, N. Desai, et al., *Comput.Phys.Commun.* **191**, 159 (2015), 1410.3012.
- [29] M. Cacciari, S. Frixione, N. Houdeau, M. L. Mangano, P. Nason, et al., *JHEP* **1210**, 137 (2012), 1205.6344.
- [30] S. Frixione and B. R. Webber, *JHEP* **0206**, 029 (2002), hep-ph/0204244.
- [31] J. Alwall, R. Frederix, S. Frixione, V. Hirschi, F. Maltoni, et al., *JHEP* **1407**, 079 (2014), 1405.0301.
- [32] M. Cacciari, M. Greco, and P. Nason, *JHEP* **9805**, 007 (1998), hep-ph/9803400.
- [33] M. Cacciari, S. Frixione, and P. Nason, *JHEP* **0103**, 006 (2001), hep-ph/0102134.
- [34] A. Buckley, J. Ferrando, S. Lloyd, K. Nordström, B. Page, et al., *Eur.Phys.J.* **C75**, 132 (2015), 1412.7420.
- [35] D. de Florian et al. (The LHC Higgs Cross Section Working Group) (2016), 1610.07922.
- [36] R. D. Ball et al. (The NNPDF), *Nucl. Phys.* **B849**, 112 (2011), 1012.0836.
- [37] R. D. Ball, V. Bertone, F. Cerutti, L. Del Debbio, S. Forte, et al., *Nucl.Phys.* **B855**, 608 (2012), 1108.1758.
- [38] M. Czakon, P. Fiedler, D. Heymes, and A. Mitov, *JHEP* **05**, 034 (2016), 1601.05375.
- [39] V. Bertone, S. Carrazza, and J. Rojo, *Comput.Phys.Commun.* **185**, 1647 (2014), 1310.1394.
- [40] S. Forte, E. Laenen, P. Nason, and J. Rojo, *Nucl. Phys.* **B834**, 116 (2010), 1001.2312.
- [41] J. Rojo and F. Caola (2009), 0906.2079.
- [42] M. G. Aartsen et al. (IceCube) (2016), 1607.05886.
- [43] S. Adrian-Martinez et al. (KM3Net), *J. Phys.* **G43**, 084001 (2016), 1601.07459.
- [44] R. D. Ball and S. Forte, *Phys. Lett.* **B335**, 77 (1994), hep-ph/9405320.
- [45] J. L. Albacete, J. I. Illana, and A. Soto-Ontoso, *Phys. Rev.* **D92**, 014027 (2015), 1505.06583.
- [46] A. Connolly, R. S. Thorne, and D. Waters, *Phys. Rev.* **D83**, 113009 (2011), 1102.0691.
- [47] L. A. Anchordoqui et al., *JHEAp* **1-2**, 1 (2014), 1312.6587.
- [48] S. P. Jones, A. D. Martin, M. G. Ryskin, and T. Teubner (2016), 1610.02272.
- [49] D. d’Enterria and J. Rojo, *Nucl.Phys.* **B860**, 311 (2012), 1202.1762.
- [50] T. Peitzmann (ALICE FoCal) (2016), 1607.01673.